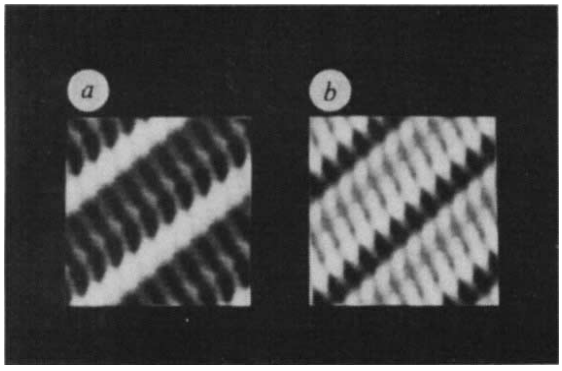


FIG. 4 *a*, STM image of PYP 909, showing the bright aromatic portions of the molecules and the dimmer aliphatic parts. *b*, Identical image of PYP 909, except that the contrast has been reversed. The two images were taken under identical tunnelling parameters, and about 10 min apart.

modulate the work function more weakly. They therefore appear dimmer in the images. Functional groups which are electronically as dissimilar as benzene and cyclohexane can have similar contrast when imaged by the STM, because their polarizabilities are comparable[16]. Finally, the contrast also depends on the size and extent of the dipole layer of the particular substrate and on the ability of the adsorbed molecules to modify it.

We note that according to equations (3) and (4), the observed contrast can change, or even reverse, depending on the sign and magnitude of the external electric field applied by STM tip (we estimate that the field that is due to the STM is of the same order as that from the polarized adsorbate, $\sim 10^7\ V\ m^{-1}$). The STM images generated can therefore depend on tip voltage and mistakenly appear to contain spectroscopic information. The contrast can also change if the tip changes its shape or absorbs dielectric material. This effect is demonstrated in Fig. 4*a* and *b*, which shows STM images of the liquid crystal PYP 909. Figure 4*a* displays the usual contrast seen when imaging this molecule: the central aromatic core appears brighter than the aliphatic tails. For approximately 5% of the time, however, the molecule is imaged with the reverse contrast, as shown in Fig. 4*b*. We attribute the reversal to the temporary adsorption of a molecule on the tip, causing a change in the electric ffeld across the liquid-crystal monolayer.

To date, we have imaged five widely divergent types of liquid-crystal molecules, all with near-atomic resolution (see also ref. 3). We conclude that the contrast mechanism for imaging physisorbed molecules is the modulation of the substrate work function by the polarizable adsorbate. The modulation is sufficiently local to enable the STM to resolve individual molecules spaced by 5 Å and to distinguish between the different functional groups within the molecules. □

Received 25 November 1988; accepted 25 January 1989.

1. Binnig, G. & Rohrer, H. *Helv. phys. Acta* **55**, 726–735 (1982).
2. Binnig, G. & Rohrer, H. *IBM Jl. Res. Dev.* **30**, 355–369 (1986).
3. Foster, J. S. & Frommer, J. E. *Nature* **333**, 542–545 (1988).
4. Brownsey, G. J. & Leadbetter, A. J. *Phys. Rev. Lett.* **44**, 1608–1611 (1980).
5. Leadbetter, A. J., Frost, J. C., Gaughan, J. P., Gray, G. W. & Mosley, A. *J. Physique* **40**, 375–380 (1979).
6. Lang, N. D. *Phys. Rev.* B**37**, 10395–10398 (1988).
7. Weber, R. E. & Peria, W. T. *Surf. Sci.* **14**, 13–38 (1969).
8. Antoniewicz, P. R. *Phys. Rev. Lett.* **32**, 1424–1425 (1974).
9. Antoniewicz, P. R. *Surf. Sci.* **52**, 703–708 (1975).
10. Topping, J. *Proc. R. Soc.* A**114**, 67–72 (1927).
11. Robrieux, B., Faure, R. & Dussaulcy, J. P. *C.R. Acad. Sci. Ser. B* **278**, 659–662 (1974).
12. Battezzatti, L., Pisani, C. & Ricca, F. *J. chem. Soc.* **71**, 1629–1639 (1975).
13. Gland, J. L. & Somorjai, G. A. *Surf. Sci.* **38**, 157–186 (1973).
14. Gimzewski, J. K. & Moller, R. *Phys. Rev.* B**36**, 1284–1287.
15. Lang, N. D. *Phys. Rev.* B**36**, 8173–8176 (1987).
16. *CRC Handbook of Chemistry and Physics* 66th Edn, E-70 (1985).
17. Crepeau, R. H. & Fram, E. K. *Ultramicroscopy* **16**, 7–17 (1981).

ACKNOWLEDGEMENTS. We thank F. Allen, P. Bagus, E. Barrall, P. Hansma, M. Miller, H. Ohtani and C. F. Quate for helpful discussions.

# Evidence for sinking of small particles into substrates and implications for heterogeneous catalysis

**P. M. Ajayan & L. D. Marks**

Department of Materials Science and Engineering, Northwestern University, Evanston, Illinois 60208, USA

**THE shapes and structures of small metal particles (1–10 nm in size) supported on oxide substrates and the effect of substrate–particle interactions in such systems are of substantial importance for heterogeneous catalysis. Here we present, for the first time, experimental evidence using atomic-resolution electron microscopy of gold clusters on MgO smoke particles, which shows that a small particle sitting on a substrate may be thermodynamically unstable and can 'sink' into the substrate. A simple theoretical model is proposed to explain this effect. The results may be of importance in small-particle catalyst systems. The stability of the particle with respect to sinking, and hence reactivity, can be changed by chemisorption of impurities, which will change the surface free energies. A plausible model of catalyst deactivation is that the particle sinks diffusively into the substrate in the course of time. Regeneration of the catalyst could require changing the surface free energy by chemisorption, causing the particle to float back onto the substrate surface.**

The structure of a small particle may not resemble the structure of the same bulk material because the large surface-to-volume ratio gives rise to a large surface-energy contribution to the total energy. The shape of a small particle is highly surface-energy-dependent and can be estimated by the Curie–Wulff construction[1,2]. Energetically stable configurations at small sizes take the form of icosahedra and particles that are multiply twinned; as demonstrated recently, the particles can undergo quasi-melting transformations between various forms[3]. What happens when such a particle is placed on top of a relatively large substrate, as one finds, for example, in heterogeneous catalysts? The resulting configurations will be determined by the relative surface free energies of the facets of the particle and the substrate, and the interfacial free energy. Theories for particle shapes on a substrate and the associated wetting transitions have been

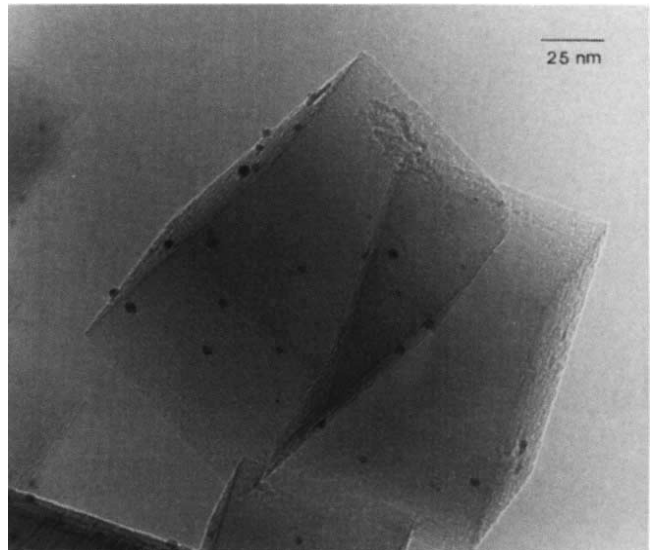


FIG. 1 Low-magnification electron-microscope image showing cuboids of transparent MgO smoke particles with gold microclusters on the surfaces.

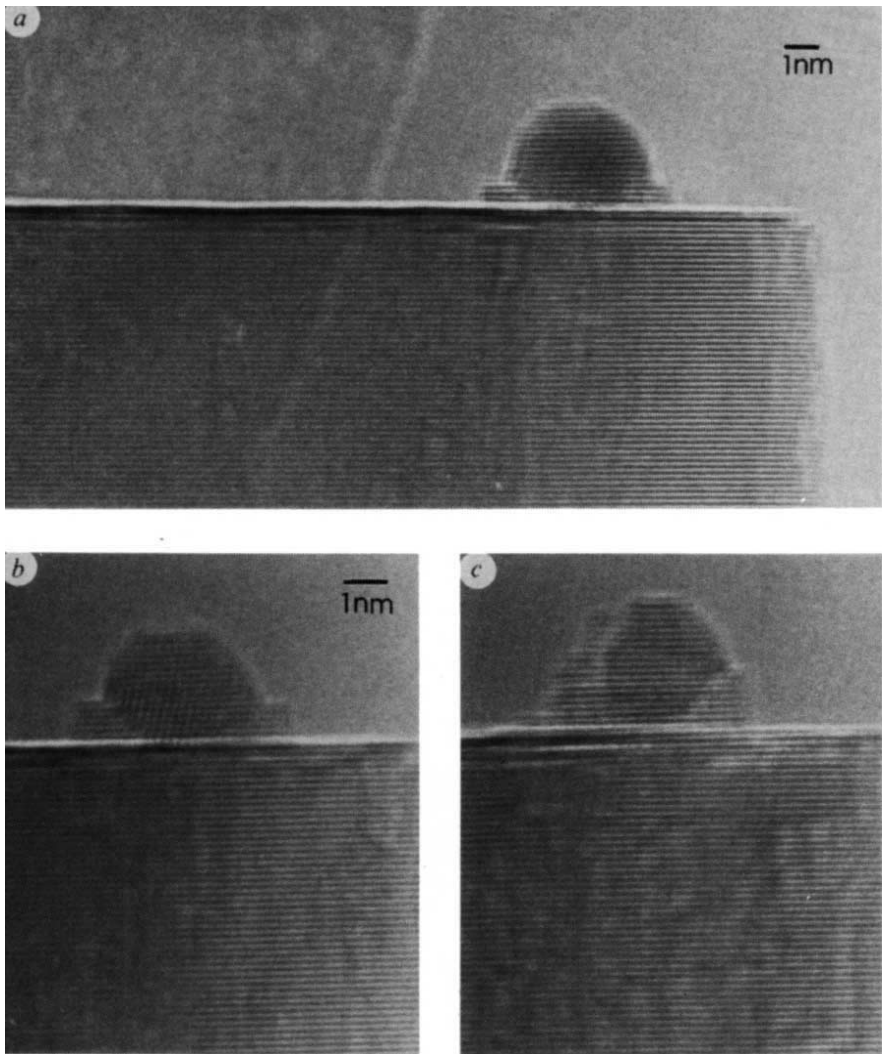


FIG. 2 *a*, High-resolution image of a gold particle on an MgO surface. Layers of MgO form on the particle following irradiation with an electron beam. The lattice layers in the substrate correspond to the (200) atomic planes. *b* and *c* show the same particle after low-flux electron irradiation for 10 and 60 min respectively. The particle sinks into the substrate and also undergoes some shear.

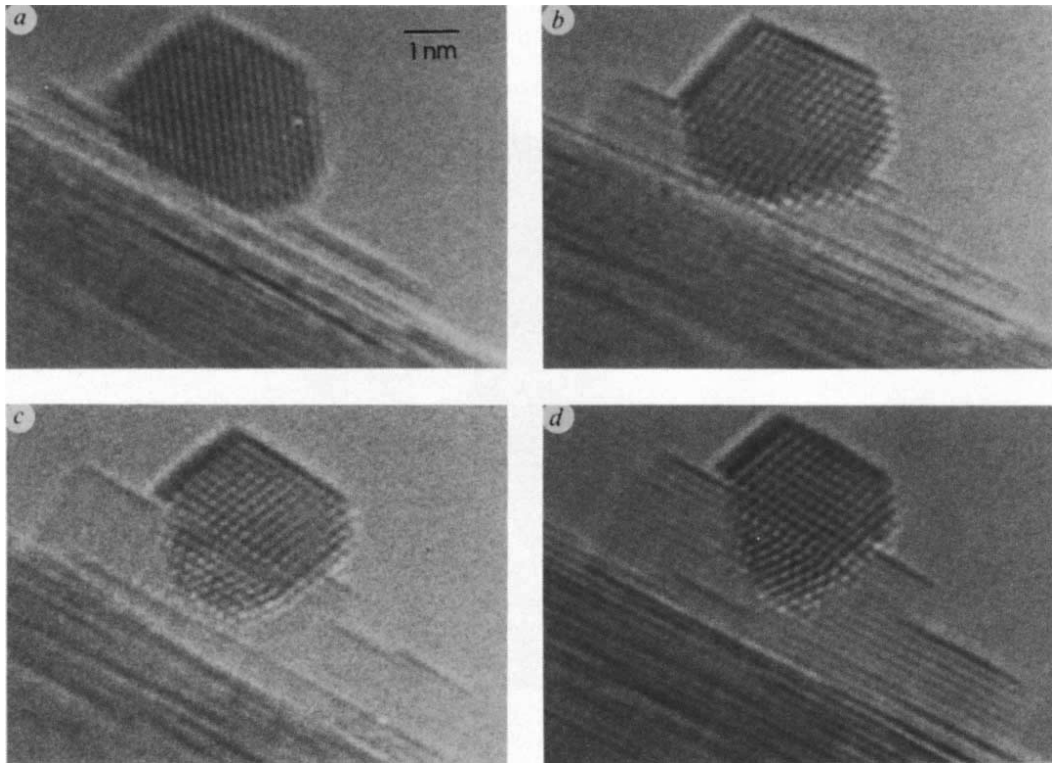


FIG. 3 Irradiation sequence of a gold particle on an MgO surface. *a*, Initial particle. *b*, After 10 min under low flux. *c*, After 30 min under low flux. Note that a twin boundary has formed in the lower part of the particle. *d*, After an additional 10 min of high-flux irradiation.

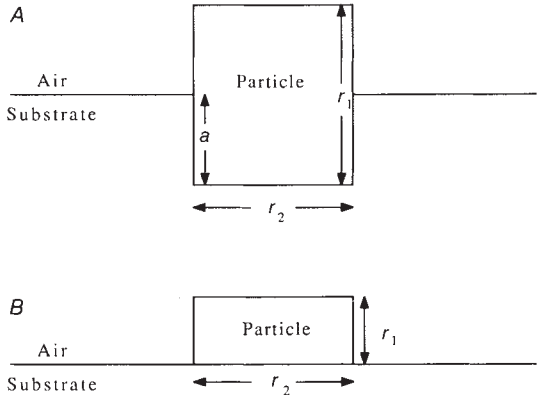


FIG. 4 *A*, Schematic diagram of a particle that is partly immersed in the substrate. *B*, A particle on a planar substrate. We assume for simplicity that the particle is of unit length normal to the figure and that the substrate surface is semi-infinite.

developed[4–6], but only for planar interfaces. If the interface is not flat, the particle can either 'sink' into the substrate or 'float' on top.

Our experiments have studied the dispersion of microclusters of gold, prepared by reduction of organometallics[7], onto magnesium oxide smoke particles (formed by burning magnesium ribbon in air). The specimens were imaged in a Hitachi H-9000 high-resolution electron microscope, operating at an accelerating voltage of 300 kV, which is capable of resolving individual atoms. The MgO particles, a few times 10 nm to a few micrometres in size, are cuboids with predominantly low-energy (100) facets, and the gold particles are found to decorate the surface of these cuboids (Fig. 1).

The experimental observations are shown in Figs 2 and 3. Figure 2 shows high-magnification images of a gold cluster on an MgO particle before and after being irradiated under low-electron-flux conditions ($\sim$100 A cm$^{-2}$). On irradiation, the substrate engulfs the particle, or alternatively the particle sinks into the substrate. The lattice spacings of the overlayer that forms on the particle match the (200) spacings of the MgO substrate. Figure 3 shows a similar irradiation sequence of another particle, taken under atomic resolution, under low- and high-electron-flux conditions (the two fluxes differ by a factor of $\sim$50). In general it appears that sinking occurs faster at higher fluxes. Observations on many different particles confirm these results. In most cases a sinking particle orientates epitaxially to the engulfing substrate and can form defects, such as the twin boundary seen in Figs 3*c* and *d*. If the particle is epitaxial with respect to the substrate, sinking occurs much faster, whereas if there is some contamination on the particle the process may be retarded or even halted. Using the relation $l=\sqrt{2Dt}$, where $l$ is the diffusion length and $t$ the diffusion time, we obtain an estimate of the diffusion coefficient $D$ for the encapsulation process of $10^{-17}$ cm$^2$ s$^{-1}$, a value comparable to that found in SMSI (strong metal-substrate-interaction) systems[8–10]. We believe that here the electron irradiation, rather than thermal effects, provides the driving force for diffusion; this is consistent with the observation, during irradiation, of roughening of the MgO surface far from the gold clusters.

A simple model can be used to explain these phenomena. Figure 4*A* shows schematically a particle that is partially immersed in a substrate. Assuming that the strain energies at the interface are negligible compared with the surface energies (which holds if the interface is epitaxial) we can write the potential energy of the system as:

$$E=(r_2+2a)(\gamma_s^p+\gamma_s^{sub}+\gamma_I)+(2r_1+r_2-2a)\gamma_s^p-r_2\gamma_s^{sub} \quad (1)$$

Here $\gamma_s^p$ is the energy of the particle-vapour interface, $\gamma_s^{sub}$ that of the substrate-vapour interface, and $\gamma_I$ the bonding energy of the interface; the distances $r_1$, $r_2$ and $a$ are defined in Fig. 4*A*. By definition, $\gamma_s^p$ and $\gamma_s^{sub}$ are positive and $\gamma_I$, the energy released when the two surfaces are brought together, is negative. The change in total energy with respect to $a$ is

$$\partial E/\partial a=2(\gamma_s^{sub}+\gamma_I) \quad (2)$$

If $\partial E/\partial a<0$ (corresponding to a particle that forms a high-energy interface on a low-energy substrate facet, as may be the case here) the particle will sink; if $\partial E/\partial a>0$, it will float. The system is thus thermodynamically unstable with respect to sinking or floating. Note that if the particle and the substrate consist of the same material the problem reduces to that of conventional sintering, and sinking becomes equivalent to heterogeneous sintering or Ostwald ripening. For a planar substrate surface (Fig. 4*B*), the energy balance is obtained similarly, and gives the criteria for wetting:

$$2\gamma_s^p+\gamma_I<0 \quad \text{Particle wets} \quad (3)$$

$$2\gamma_s^{sub}+\gamma_I<0 \quad \text{Substrate wets} \quad (4)$$

Note that the propensity of a particle to sink will be sensitive to changes in the surface free energies, as might be induced, for example, by chemisorption of impurities. □

Received 2 November 1988; accepted 31 January 1989.

1. Herring, C. *Structure and Properties of Solid Surfaces* (eds Gomer, R. & Smith, C. S.) 5–72 (Univ. of Chicago Press, 1953).
2. Rottman, C. & Wortis, M. *Phys. Rep.* **103**, 59–79 (1984).
3. Ajayan, P. M. & Marks, L. D. *Phys. Rev. Lett.* **60**, 585–587 (1988).
4. Winterbottom, W. L. *Acta Met.* **15**, 303–310 (1967).
5. Pillar, R. M. & Nuttig, J. *Phil. Mag.* **16**, 181–188 (1967).
6. Heyraud, J. C. & Metois, J. J. *Acta Met.* **28**, 1789–1797 (1980).
7. Teo, B. K. & Keating, K. *J. Am. chem. Soc.* **106**, 2224–2226 (1984).
8. Tauster, S. J. *et al. J. Am. chem. Soc.* **100**, 170–175 (1978).
9. Chen, Bor-Her. & White, J. M. *J. phys. Chem.* **86**, 3534–3541 (1982).
10. Spencer, M. S. *J. Catal.* **93**, 216–223 (1985).

ACKNOWLEDGEMENTS. We acknowledge funding by the NSF.

# Stress-induced Al–Cr zoning of spinel in deformed peridotites

**Kazuhito Ozawa**

Geological Institute, Faculty of Science, University of Tokyo, Tokyo 113, Japan

**DEFORMATION is one of the principal processes governing the microstructure of solid materials, but it may also affect their chemistries[1–5]. Chemical unmixing in non-hydrostatically stressed, initially homogeneous multicomponent solids has been predicted to occur during diffusion creep[5,6]. Yet there has been no report of chemical zoning induced by diffusion creep in either naturally or experimentally deformed solid-solution materials. Here I report Al–Cr zoning in elongated Cr-spinel ($(Cr, Al, Fe^{3+})_2(Mg, Fe^{2+})O_4$) grains from deformed peridotites and chromitites, which shows a consistent orientation of Al-rich and Al-poor regions with respect to the lineation and the shape of the spinel grain. I interpret this zoning as having been induced by deformation, and it is most reasonably explained by stress-directed lattice diffusion of Al and Cr.**

I have determined the distribution of elements in spinel grains of spinel peridotites from the Miyamori ophiolitic complex and the Horoman ultramafic complex in north-east Japan, and in a chromitite from the Oman ophiolite, by electron-probe microanalysis (JEOL JCMA 733 Mk-II). In the analyses, the specimen stage was automatically driven at 20–40 μm s$^{-1}$ (50 ms counting time at each point and 1 or 2 μm pixel size). The total number of pixels for each spinel analysis ranged from 200 × 200 to 300 × 400.